Quantification of healthy and atretic germ cells and follicles in the developing and post-natal ovary of the South American plains vizcacha, *Lagostomus maximus*: evidence of continuous rise of the germinal reserve

P I F Inserra*, N P Leopardo*, M A Willis, A L Freysselinard and A D Vitullo

Departamento de Ciencias Biomédicas y Biotecnológicas, Centro de Estudios Biomédicos, Biotecnológicos, Ambientales y Diagnóstico (CEBBAD), Universidad Maimónides, Hidalgo 775, C1405BCK, Ciudad Autónoma de Buenos Aires, Buenos Aires, Argentina

Correspondence should be addressed to A D Vitullo; Email: vitullo.alfredo@maimonides.edu

*(P I F Inserra and N P Leopardo contributed equally to this work)

Abstract

The female germ line in mammals is subjected to massive cell death that eliminates 60–85% of the germinal reserve by birth and continues from birth to adulthood until the exhaustion of the germinal pool. Germ cell demise occurs mainly through apoptosis by means of a biased expression in favour of pro-apoptotic members of the *BCL2* gene family. By contrast, the South American plains vizcacha, *Lagostomus maximus*, exhibits sustained expression of the anti-apoptotic *BCL2* gene throughout gestation and a low incidence of germ cell apoptosis. This led to the proposal that, in the absence of death mechanisms other than apoptosis, the female germ line should increase continuously from foetal life until after birth. In this study, we quantified all healthy germ cells and follicles in the ovaries of *L. maximus* from early foetal life to day 60 after birth using unbiased stereological methods and detected apoptosis by labelling with TUNEL assay. The healthy germ cell population increased continuously from early-developing ovary reaching a 50 times higher population number by the end of gestation. TUNEL-positive germ cells were <0.5% of the germ cell number, except at mid-gestation (3.62%). Mitotic proliferation, entrance into prophase I stage and primordial follicle formation occurred as overlapping processes from early pregnancy to birth. Germ cell number remained constant in early post-natal life, but a remnant population of non-follicular VASA- and PCNA-positive germ cells still persisted at post-natal day 60. *L. maximus* is the first mammal so far described in which female germ line develops in the absence of constitutive massive germ cell elimination.

Free Spanish abstract

Introduction

In mammals, oogenesis starts early in foetal life when primordial germ cells (PGCs) transform into actively proliferating oogonia in the developing ovary and then enter meiotic prophase I stage. Before birth or early after birth, oocytes in diplotene stage enter a quiescent state known as dictyate, in which they remain arrested, sometimes for years or decades depending on the species, until just before ovulation (Speed 1982). This unidirectional sequence of changes that produce a finite pool of dictyate-arrested oocytes with no persistence of PGCs or oogonia in the adult life has been a matter of discussion throughout the 20th century since Pearl & Schoppe (1921) had proposed that post-natal oogenesis might occur in the mammalian adult ovary. Reviewing the subject, Zuckerman (1951) leaned on the absence of oogenesis in the mature mammalian ovary, a perspective that was widely accepted by researchers until now. More recently, the finding of a small population of germ-line stem cells in the ovary of the adult laboratory mouse that could help to maintain the oocyte reserve by *de novo* oogenesis in post-natal life has once again fuelled the debate of whether or not post-natal oogenesis takes place in the mammalian ovary (Johnson *et al*. 2004). Since then, evidence for and against *de novo* oogenesis has accumulated, and the subject still remains an open question (Tilly *et al*. 2009, Gougeon 2010).

By the time it was accepted that mammals are born with a finite, non-renewable oocyte pool, studies in the human ovary had established another characteristic trait of mammalian oogenesis, the existence of constitutive

massive germ cell death through cell attrition in foetal life and follicular atresia in the ovary in adulthood (Baker 1963, Baker & Franchi 1967). After colonising the genital ridges during early foetal life, human PGCs actively proliferate to produce by gestation week 20 around 7×10^{6} primary oocytes. However, massive germ cell attrition takes place throughout the foetal development period, leading the ovary to contain just around 10^{6} primordial follicles at birth (Baker 1963, Forabosco et al. 1991). Thus, 85% of the original oocyte pool is lost during gestation, and germ cell demise continues after birth resulting in 400 000 germ cells at puberty, a wasteful cellular loss of almost 95% of the potential oocyte population reached at mid-gestation. Comparable germ cell demise has also been found to occur in other mammals. In rats, germ cell number decreases by two-thirds from the onset of meiosis to 48 h after birth (Hirshfield 1991); in mice, 66% of the original oogonia are decimated by the end of gestation (Flaws et al. 2001). Massive germ cell demise occurs through cell death mechanisms that mainly rely on apoptosis (Coucouvanis et al. 1993, Hsueh et al. 1996, Tilly 1996a, 1996b, Tilly et al. 1997) by means of a concerted spatial–temporal expression of anti- and pro-apoptotic genes belonging to the *BCL2* gene family, among which *BCL2*, *BAX* and *BCL2L1* (*BCL-X*) genes seem to play an important role (Albamonte et al. 2008). For instance, it has been observed that the expression of *BAX* is normally enhanced in the mammalian ovary, whereas BCL2 protein is present in low amounts or is completely undetected (De Felici 1999, Kim & Tilly 2004, De Felici et al. 2005). The enhanced expression of pro-apoptotic *BAX* gene gives support to the high rate of apoptosis characterising the mammalian ovary and has been experimentally supported by showing that *Bcl2*- and *Bax*-knockout mice have decreased or increased primordial follicle reserve respectively (Knudson et al. 1995, Ratts et al. 1995). Thus, the current state of the knowledge indicates that oogenesis in mammals, starting early in foetal life through the proliferation of PGCs and oogonia, is subjected to massive intraovarian germ cell death that eliminates one-half to two-thirds of germ cells to finally yield a finite, non-renewable pool of dictyate-arrested, follicle-enclosed oocytes at birth.

The South American plains vizcacha, *Lagostomus maximus*, is a caviomorph rodent distributed mainly in the Pampa plains of Argentina. Females exhibit the highest rate of ovulation recorded for a mammal, releasing up to 800 oocytes at each oestrus cycle (Weir 1971a). Massive polyovulation has been explained to occur as a consequence of the peculiar anatomy of the ovary characterised by a highly convoluted cortex that goes deeply into the medulla, substantially increasing the surface area for ovulation (Weir 1971b, Mossman & Duke 1973, Flamini et al. 2009, Espinosa et al. 2011). In addition to the increased ovulation area, we observed sustained expression of apoptosis-inhibiting *BCL2* gene

and low expression of apoptosis-inducing *BAX* gene, which may be responsible for suppressing apoptosis-dependent follicular atresia in the ovary of the adult female (Jensen et al. 2006). Moreover, sustained *BCL2* expression is a constitutive ovary-specific trait that may also play an important role in decreased apoptosis-dependent germ cell attrition throughout the foetal development period (Leopardo et al. 2011). In contrast to what is expected to occur in the developing mammalian ovary, the detection of low levels of apoptosis-dependent germ cell attrition suggests that germ cell proliferation in *L. maximus* might not be counterbalanced through massive elimination, leading to a continuous rise in germ cell number, unless death mechanisms other than apoptosis are at play. To validate or discard this proposal, the aim of the present study was to quantify healthy germ cells and follicles in the developing and post-natal ovary of *L. maximus* using unbiased stereological methods (Gundersen 1986). In addition, TUNEL assay was used to quantify the incidence of apoptosis and meiotic prophase I progression in the foetal and post-natal ovaries was also characterised.

Materials and methods

Animals

The experimental protocol described herein was reviewed and authorised by the Institutional Committee on the Use and Care of Experimental Animals (CICUAE, Universidad Maimónides). The captured animals were handled and killed in accordance with the standards defined in the Guide for the Care and Use of Laboratory Animals (CCAC 2002) and Guidelines on the Care and Use of Wildlife (CCAC 2003) from the Canadian Council of Animal Care. Pregnant plains vizcachas, *L. maximus*, were captured from a resident natural population at the Estación de Cría de Animales Silvestres (ECAS), Villa Elisa, Buenos Aires, Argentina. A total of 15 pregnant adult females were captured at three different time points during the breeding season, which extends from March to September. The animals were captured using live traps located at the entrance of the burrows. Female gestational age was estimated on the basis of capture time, foetal development, and foetal weight and crown–heel length as reported previously (Leopardo et al. 2011). A total of 15 female foetuses, five from each gestational time point (early, mid and late gestation), were recovered from pregnant females. Nine foetuses, three from each time point, were used for cell counting; the remaining six, two from each time point, were used for meiotic analysis. Only the foetuses located nearest to the cervix were included in this analysis, as it is known that they are the only ones that develop to term; the remaining foetuses that are anteriorly implanted are selectively aborted (Weir 1971a, Jensen et al. 2008). Early-gestating females, captured in late May, had foetuses corresponding to 50 ± 15 gestation days; mid-gestating females, captured in late June/early July, had foetuses corresponding to 90 ± 15 gestation days; and late-gestating females, captured in late July/early August, had well-developed perinatal foetuses

corresponding to 140 ± 15 gestation days. Additionally, the ovaries collected from three pre-pubertal females, 45–60 days old, born in the laboratory to captured late-pregnant females, were analysed.

Tissue collection and processing

The animals were anaesthetised by i.m. administration of 13.5 mg/kg body weight of ketamine chlorhydrate (Holliday Scott S.A., Buenos Aires, Argentina) and 0.6 mg/kg body weight of xylazine chlorhydrate (Richmond Laboratories, Veterinary Division, Buenos Aires, Argentina) and killed by an intracardiac injection of Euthanyl (0.5 ml/kg body weight, sodic pento-barbital and sodic diphenylhydantoin, Brouwer S.A., Buenos Aires, Argentina). Immediately after killing, the uterine horns were exposed and foetuses were removed for fixation. Early-gestating foetuses were entirely fixed in cold 4% neutral-buffered paraformaldehyde (PFA) for 24 h. Mid- and late-gestating foetal ovaries were removed from the foetuses and fixed in cold PFA for 24 h. Ovaries collected from pre-pubertal females were preserved in the same way. After fixation, foetal and pre-pubertal ovaries were dehydrated through a graded series of ethanol (50, 70, 95 and 100%) and embedded in paraffin. The whole embedded ovaries were serially sectioned at a thickness of 6 µm and mounted onto cleaned, coated slides (Fig. 1A). Sections of each sample selected for quantification were processed for TUNEL assay with peroxidase conversion and counterstained with haematoxylin–eosin.

TUNEL assay

Apoptosis-associated DNA fragmentation was detected by the TUNEL technique (Gavrieli *et al.* 1992) using the *in situ* Cell Death Detection Kit with peroxidase converter (Roche Diagnostics, Roche Applied Science). Mounted sections were dewaxed in xylene, rehydrated through a decreasing series of ethanol (100, 95, 70 and 50%) and PBS, permeabilised with 20 µg/ml nuclease-free Proteinase K in 10 mM Tris–HCl (Invitrogen, Life Technologies Corporation) for 30 min at 37 °C, and finally blocked for endogenous peroxidase activity with 3% hydrogen peroxide in methanol for 30 min at room temperature. The TUNEL reaction was carried out following the supplier's recommendations. The sections were incubated with the TUNEL reaction mixture (labelling solution plus the terminal transferase enzyme) for 60 min at 37 °C and checked for appropriate reaction with an Olympus BX40 microscope (Olympus Optical Corporation, Tokyo, Japan) by conventional epifluorescence with u.v. illumination. To achieve signalling conversion, endogenous IgG activity was blocked with 10% bovine foetal serum and 15% BSA (BSA Fraction V, Sigma–Aldrich, Inc.) in PBS for 60 min at room temperature. Signalling conversion was performed using converter-POD (Roche Diagnostics, Roche Applied Sciences) for 30 min at 37 °C. The conversion was visualised using the 3,3′-diamino-benzidine (DAB) Kit (SK-4100, Vector Laboratories, Burlingame, CA, USA). TUNEL-treated sections were counterstained with haematoxylin–eosin and coverslipped. To confirm negative results, TUNEL-processed and -counted sections were incubated with 10 IU/ml recombinant DNaseI (Invitrogen,

Life Technologies Corporation) in 50 mM Tris–HCl (pH 7.5), 10 mM $MgCl_2$ and 1 mg/ml BSA for 60 min at room temperature. After incubation with the enzyme, the slides were thoroughly rinsed with PBS and reprocessed for TUNEL assay. A negative control assay was carried out by omitting the terminal transferase enzyme.

Quantification of germ cell population

The total number of germinal cells and oocyte-containing follicles was determined combining the 'fractionator' sampling method – an unbiased sampling procedure based on repeated fractionation of the tissue samples with known sampling fractions (Gundersen 1986, Gundersen *et al.* 1988) – and the 'physical dissector' counting method – a stereological probe for counting or selecting objects using a pair of adjacent physical sections (Sterio 1984). Pairs of two consecutive sections were sampled, the primary section (PS) and the reference section (RS) respectively, by systematic uniform random sampling (Gundersen & Jensen 1987) with a random start between section number 1 and section number $N_{sect\ (p–p)}$, i.e. the number of sections between two PSs (Hartoft-Nielsen *et al.* 2005; Fig. 1B). Owing to differences in the size of the ovaries,
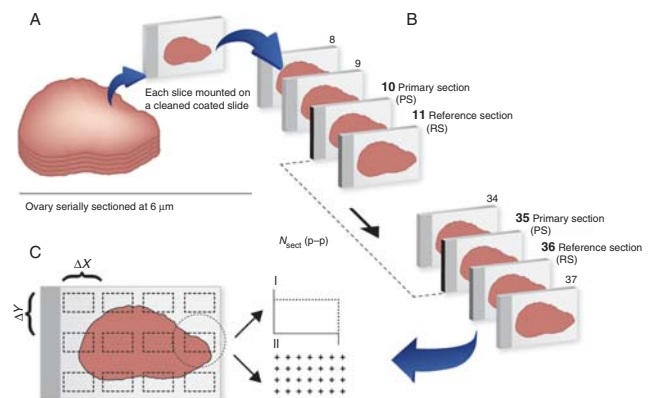
Figure 1 Tissue processing, section sampling and analysis for germ cell counting in the whole ovary. (A) Each ovary was serially sectioned at a thickness of 6 µm, and each slice was mounted onto cleaned coated slides. (B) Ovary sections were sampled by systematic uniform random sampling. Pairs of two consecutive sections were chosen with a random start within the first section and the section equivalent to $N_{sect\ (p–p)}$. $N_{sect\ (p–p)}$ was calculated dividing, in each case, the total number of sections obtained from one ovary by 10. This ensured the analysis of ten pairs of sections per ovary, distributed throughout the whole organ. For example, if $N_{sect\ (p–p)}$ is 25, we randomly selected the first consecutive pair between section 1 and section 25. If the start is, for example, section 10, we selected slides 10 and 11 as the first pair for analysis and 25 is the distance between this pair and the next one. Then, sections 10 and 11, 35 and 36, 60 and 61, 85 and 86, and so on were sampled. For each pair, the first sampled section is called the primary section (PS) and the subsequent section is called the reference section (RS). (C) Every PS sampled was systematically investigated taking areas of analysis separated by a known distance in the horizontal and vertical axes (ΔX and ΔY respectively). The values of ΔX and ΔY were kept constant for each ovarian developmental stage. Each area of analysis was investigated by applying an unbiased counting frame (CI) and a point grid (CII), a grid of systematically distributed points. The same areas of analysis were studied in the RS to avoid redundant counting.

$N_{\text{sect (p–p)}}$ was adjusted in each case to ensure the analysis of ten pairs of sections per ovary. All the PSs were systematically counted, and for each field of the PS analysed, the corresponding area on the RS was located to detect repeated germinal cells/follicles. Only those germinal cells/follicles that were completely inside the sampling frame (Fig. 1CI) and that were not repeated in the RS were counted.

An unbiased estimate of the total number of germinal cells/follicles ($N_{\text{cel/fol}}$) was obtained with the following formula: $N_{\text{cel/fol}} = \Sigma Q^- \times f_1 \times f_2$, where '$\Sigma Q^-$' is the sum of all the counted germinal cells/follicles, 'f_1' is $N_{\text{sect (p–p)}}/N_{\text{sect (p–r)}}$ (where '$N_{\text{sect (p–p)}}$' is the number of sections between two PSs and '$N_{\text{sect (p–r)}}$' is the number of sections between the PS and the RS, 1 in this case) and 'f_2' is $\Delta X \times \Delta Y/A$ (where '$\Delta X \times \Delta Y$' are the step lengths in the horizontal and vertical axes respectively and 'A' is the area of the counting frame corrected for magnification (4800 μm^2)) (Fig. 1C; Hartoft-Nielsen *et al.* 2005, Kerr *et al.* 2006). The step lengths in the 'X' and 'Y' directions were determined by a pilot study and were kept constant for each ovarian stage. All the samples were counted independently by two observers (P I F Inserra and N P Leopardo).

Determination of the germ cell composition and atretic rate

When quantifying the germinal population, the different germ cells and follicular types throughout the foetal and *post-partum* development periods were counted, and they are expressed as the percentage of the total germ cell population at each time point. Germ cells and follicles were classified according to the definitions of Hirshfield (1991) and Myers *et al.* (2004) as follows: oogonia, primary oocyte, primordial follicle, primary follicle, secondary follicle and antral follicle. TUNEL-positive oogonia, primary oocytes and follicles were also quantified to establish the rate of cell attrition.

Ovary volume and cell density

The total volume of each ovary was determined according to the Cavalieri principle with point counting (Gundersen 1986, Gundersen & Jensen 1987, Gundersen *et al.* 1988). All the PSs were analysed using a point grid, and all the points that touched the ovarian tissue were counted (Fig. 1CII). Estimates of the ovary volume (V_{ov}) were then obtained by applying the following formula: $V_{\text{ov}} = \Sigma p_{\text{ov}} \times a/p \times t$, where '$\Sigma p_{\text{ov}}$' is the number of points that touched the ovarian tissue; 'a/p' is ($\Delta X \times \Delta Y$) divided by the number of points in the grid (30 points); and 't' is the distance between two PS expressed in microns (Hartoft-Nielsen *et al.* 2005). Cell density for each time point analysed is expressed as total cell number/total ovary volume.

Immunohistochemical co-localisation of VASA and PCNA in post-natal ovaries

Ovarian sections obtained from three pre-pubertal females were dewaxed in xylene and rehydrated through a decreasing series of ethanol (100, 95 and 70%). Antigen retrieval was carried out by boiling the sections in 10 mM sodium citrate (pH 6.0) for 20 min, followed by 20 min of cooling at room temperature.

Endogenous peroxidase activity was blocked with 3% hydrogen peroxide for 20 min at room temperature. The sections were incubated with a blocking solution containing 10% goat serum in PBS (pH 7.4) for 30 min at room temperature. PCNA immunoreactivity was detected by incubating the slides overnight at 4 °C with rabbit polyclonal anti-PCNA IgG (1:250 dilution, ab-2426; Abcam, Inc., Cambridge, MA, USA). The immune reaction was revealed with biotinylated goat anti-rabbit IgG, followed by incubation with avidin–biotin complex (PK-6101, ABC Vectastain Elite Kit, Vector Laboratories). The reaction was visualised with DAB (SK-4100, DAB Kit, Vector Laboratories). After three washes of 30 min each with 0.01% Triton in PBS for 30 min, the sections were incubated with a blocking solution containing 10% rabbit serum in PBS (pH 7.4) for 30 min at room temperature. VASA immunoreactivity was detected by incubating the slides overnight at 4 °C with goat polyclonal anti-VASA IgG (1:250 dilution, SC-48707, Santa Cruz Biotechnology, Inc.). Immunoreactivity was revealed with biotinylated rabbit anti-goat IgG, followed by incubation with avidin–biotin complex (PK-6105, ABC Vectastain Elite Kit, Vector Laboratories). The reaction was visualised with DAB blue (SK-4700, DAB Kit, Vector Laboratories). Finally, the treated sections were dehydrated through a graded series of ethanol (70, 95 and 100%), cleared in Neo-Clear (Merck KGaA) and coverslipped. Staining for each antibody was repeated at least three times in separate assays for each specimen, using a minimum of two slides per assay. Repetitions of assays performed on different days confirmed that staining was reproducible. Negative control assays were carried out by omitting the primary antibody (PCNA) or pre-absorbing primary antibodies with the synthetic peptides (VASA).

Meiotic prophase I analysis

Histological paraffin sections were screened during cell counting for morphological analysis of the prophase I stages of meiosis in non-follicular primary oocytes and primordial follicle-enclosed oocytes. Oogonia in mitotic metaphase stage and primary oocytes in leptotene, zygotene, pachytene and diplotene stages of meiotic prophase I were quantified according to the nuclear staining configuration following the classification of Kurilo (1981). Leptotene nuclei exhibited a heterogeneous distribution of chromatin with patches of sharp staining due to chromosome condensation; zygotene nuclei exhibited sharp staining of fully condensed chromosomes with a typical lateral localisation within the cell; pachytene oocytes exhibited superimposed individual bivalents with maximum contraction and diplotene oocytes acquired the characteristic rounded shape with a centrally situated nucleus surrounded by a rather thick layer of cytoplasm; and chromatin exhibited a very heterogeneous sharp staining revealing bivalents remaining joined in chiasmata areas.

In addition, spread preparation was performed using ovaries obtained from six female foetuses, two for each gestational time point (early, mid and late gestation). Ovaries were placed onto cleaned slides in three drops of 0.2 M sucrose in distilled water and teased apart with needles. Large debris were removed, and the oocytes were dispersed in the drop and allowed to dry for 30 min at room temperature. Then, the

spreads were fixed for 10 min with 3.4% sucrose in PFA, washed for 1 min with PBS and air-dried. Finally, chromosome staining was carried out using the rapid colloidal silver method of Howell & Black (1980).

Statistical analysis

Results obtained during total germ cell and follicle counting as well as total ovary volume determination in each ovarian stage are expressed as means±s.d. Statistical analysis was carried out using Prism 4.0 (GraphPad Software, Inc., San Diego, CA, USA). Mean differences were analysed applying a *t*-test and considered significant when $P<0.05$.

Results

Quantification of healthy and apoptotic germ cell populations

Germ cell number in the ovaries of *L. maximus*, from early-developing to post-natal pre-pubertal stages, obtained through unbiased stereological counting is summarised in Table 1. The mean germ cell number± s.d. in the early-developing ovaries was 56 125±13 322, exhibited a significant 20-fold increase of 1 078 667± 156 886 at mid-gestation and continued to increase significantly up to 3 148 688±425 768 by the end of gestation. After birth, germ cell number in 45–60-day-old ovaries continued to increase, reaching 3 611 250± 351 061, but exhibited no significant differences compared with that in late-developing ovaries. Ovary volume increased significantly throughout gestation, exhibiting a more than 100 times bigger value from early gestation to late gestation (Table 1). Volume increased asynchronously to germ cell number, as reflected in germ cell density, which peaked at mid-gestation (Table 1). From early-developing to post-natal pre-pubertal ovaries, apoptosis was <0.5% of the total germ cell number, except at mid-gestation, when it reached its highest value, 3.62% (Table 1).

Quantitative composition of the germ cell and follicle population

The distribution of oogonia, primary oocytes at prophase I, primordial follicles and follicles at later stages of development is summarised in Table 2. Early-developing ovaries were entirely represented by oogonia (Table 2), most of them at interphase (Fig. 2A), with apoptotic germ cells being detected at very low levels (0.11%; Table 2 and Fig. 2B). Oogonia were still abundant at mid-gestation, representing around 64% of the total germ cell population (Table 2). The remaining 36% of the germ cell population was mainly represented by non-follicular primary oocytes that had entered prophase I (Table 2 and Fig. 2C). Oocytes at mid-gestation exhibited the highest apoptosis rate (3.62%) detected throughout the female germ-line development period (Table 2 and Fig. 2D). By the end of gestation, oogonia were significantly reduced in number, representing 4.65% of the total population (Table 2). The majority of germ cells (95.31%) were found as primordial follicle-enclosed primary oocytes (Fig. 2E) and <0.5% as detectable apoptotic germ cells (Table 2 and Fig. 2F).

After birth, 45–60-day-old pre-pubertal ovaries comprised an abundant primordial resting reserve of around 83% of the total population (Table 2). A proportion of primordial follicles (14.09%) had already left the resting reserve to enter the growing pool as primary, secondary and early-antral follicles (Table 2 and Fig. 3A) in which very occasional apoptotic follicles were found (Fig. 3B). A small population of non-follicular oogonia (3.22%) was still detectable (Table 2). The majority of non-follicular germ cells were found near the surface epithelium or in the surface epithelium proper as oogonia-like cells (Fig. 3C and D) and oocytes starting to associate with pre-granulosa cells forming incipient primordial follicles and exhibiting typical chromatin staining of meiotic prophase I (Fig. 3E). No germ cells were detected in the periovarian space. Oogonia-like cells and oocytes starting to associate with somatic cells were identified as VASA positive, and they exhibited a proliferative state as revealed by PCNA-positive staining (Fig. 3C). Very low levels of apoptosis were detected in the post-natal ovaries (0.48%), distributed almost equally among resting follicles and follicles that had entered the growing reserve (Table 2). It is worth noting that apoptosis in follicles that had entered the growing pool (primary and secondary follicles) was detected in granulosa cells (Fig. 3B).

Table 1 Total germ cell number, ovary volume and apoptosis rate in *Lagostomus maximus* throughout the foetal and early post-natal development periods.

Development (days)	Germ cell number (per ovary)	Ovary volume (mm³)	Germ cell density (cell/mm³)	Total apoptosis (%)
Pregnancy				
Early (50±15)	56 125±13 322[A]	0.15±0.01[A]	∼375 000	0.11
Mid (90±15)	1 078 667±156 886[B]	1.37±0.27[B]	∼875 000	3.62
Late (140±15)	3 148 688±425 768[C]	16.88±1.67[C]	∼185 000	0.40
Pre-pubertal (45–60[a])	3 611 250±351 061[C]	22.98±2.37[D]	∼155 000	0.48

Data are expressed as means±s.d. Different capital letters following values indicate statistical significance ($P<0.05$).
[a]Days *post-partum*.

Table 2 Germ cell composition in the ovary of *Lagostomus maximus* throughout the foetal and early post-natal development periods.

Development (days)	Oogonia				Oocytes I			Primordial follicles			Primary follicles		Secondary follicles		Antral follicles	
	In	Mi	Ap	Total	Me	Ap	Total	Me	Ap	Total	Ap	Total	Ap	Total	Ap	Total
Pregnancy																
Early (50±15)	97.83	2.06	0.11	100	–	–	–	–	–	–	–	–	–	–	–	–
Mid (90±15)	61.77	2.09	0.00	63.86	32.52	3.62	36.14	–	–	–	–	–	–	–	–	–
Late (140±15)	4.65	0.04	0.00	4.69	–	–	–	94.91	0.40	95.31	–	–	–	–	–	–
Pre-pubertal (45–60[a])	3.22	0.05	0.00	3.27	–	–	–	82.66	0.20	82.92	0.02	7.92	0.26	5.19	0.00	0.70

Data are expressed as percentage. In, interphase; Mi, mitotic metaphase; Ap, apoptosis; Me, meiotic prophase I.
[a]Days *post-partum*.

Meiotic progression in the developing and post-natal ovary of L. maximus

The progression of meiotic prophase I is summarised in Fig. 4. Early-developing ovaries, mostly comprising oogonia, did not exhibit distinguishable meiotic prophase I stages. At mid-gestation, oocytes were mainly found in leptotene stage (Fig. 4I), representing 27.86% of the total germ cell count, and in a lesser proportion in zygotene (2.85%) and pachytene (1.78%) stages (Fig. 4II). At late gestation, leptotene oocytes became undetectable and oocytes were mainly found in diplotene (64.63%) and pachytene (25.69%) stages as well as a remaining 4.95% still in zygotene stage (Fig. 4II). Pre-pubertal ovaries exhibited a distribution of oocytes in prophase I stage comparable to late-developing ovaries, with 64.74% being in diplotene stage, 17.63% in pachytene stage and a very few (0.29%) still in zygotene stage (Fig. 4II). Silver-stained spread preparations confirmed the presence of the different stages of meiotic prophase I (Fig. 4III).

Discussion

This study demonstrates that mean germ cell number per ovary increases continuously from the early development period up to 45–60 days after birth in the South American plains vizcacha, *L. maximus*, with little cell loss through apoptosis. This quantitative estimate based on unbiased stereological methods supports the assumption that the sustained expression of apoptosis-inhibiting *BCL2* gene and the low or absent detection of apoptosis-inducing *BAX* gene preclude massive germ cell demise by greatly reducing apoptosis (Jensen *et al.* 2006, Leopardo *et al.* 2011). Moreover, it also shows that the post-natal ovaries of *L. maximus* still have a proliferating germ cell population with persistence of oogonia and primordial follicle-enclosed oocytes in meiotic prophase I stage, mainly located nearest to the surface epithelium.

As far as we could track in the literature, *L. maximus* is the first mammal so far described in which the female germ line develops in the absence of constitutive massive germ cell elimination. Studies in mice, rats, humans and other mammals have shown that genetically regulated death mechanisms are responsible for eliminating 60–95% of newly formed oocytes from early foetal ovaries to puberty and appear to be a developmental pattern intrinsic to the mammalian ovary (Baker 1963, Hirshfield 1991, Flaws *et al.* 2001). Our estimate of the mean number of healthy oogonia, oocytes and follicles from early-developing ovaries, around 50 days post-coitum (dpc), to the end of gestation, 155 dpc, shows an increase of more than 50 times in the healthy germ cell population of *L. maximus*. Beginning with an endowment of ∼56 000 oogonia at 50 dpc, total germ cell number increases to around 3 150 000 by the end of
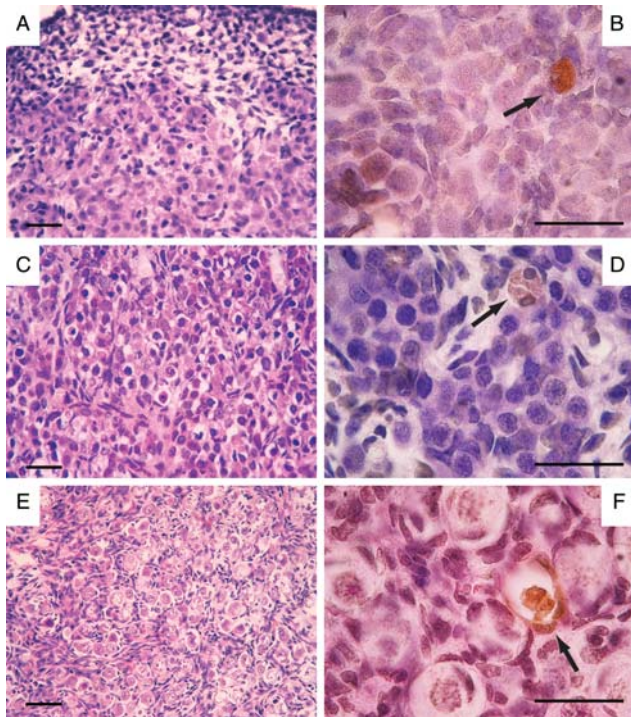
Figure 2 General histology and apoptosis detection by TUNEL assay throughout the foetal development period in the ovary of *Lagostomus maximus*. (A) Illustrative histological view of the early-developing foetal ovary exhibiting an abundance of oogonia. (B) Occasional oogonia undergoing apoptosis in early-developing foetal ovary (arrow). (C) Mid-developing ovary displaying oogonia and primary oocytes. (D) Rare germ cells in apoptosis detected in mid-gestation ovary (arrow). (E) Late-developing foetal ovary dominated by primordial follicles in which oocytes are still in prophase I stage. (F) Detection of apoptotic germ cells continued to be rare at late gestation; note that the TUNEL-positive signal in the primordial follicle involved both the oocyte and pre-granulosa somatic cells (arrow). (A, C and E) Haematoxylin–eosin staining and (B, D and F) POD-converted TUNEL assay, counterstained with haematoxylin (see Materials and methods). Bar, 20 μm.

gestation. Rare germ cells in attrition were evident in haematoxylin–eosin-stained samples, and the detection of germ cells undergoing last steps in apoptosis revealed by the TUNEL assay never surpassed 4% of the entire germinal population.

Although mechanisms of germ cell demise other than apoptosis cannot be excluded, it does not seem that any of them could affect the growing tendency of germ line in the ovaries of *L. maximus*. In both human and mouse ovaries, it has been shown that oocyte expulsion from the ovary surface contributes to the reduction of germ cell population in foetal and newborn ovaries (Peters 1969, Hiura & Fujita 1977, Wordinger *et al*. 1990, Motta *et al*. 1997, 2003). The contribution of germ cell exfoliation to the periovarian space in newborn mouse has been estimated to be 5–10% (Byskov & Rasmussen 1973), a figure that rises up to 25% loss from days 1 to 7 after birth when a more accurate stereological counting method is used (Kerr *et al*. 2006). We did not detect

oocytes in the periovarian space, although we did detect them in the surface epithelium of the post-natal ovaries of *L. maximus*. Oocytes with or without associated somatic cells lying in the surface epithelium may represent germ cells exiting the ovaries via exfoliation (Kerr *et al*. 2006). In any case, if surface germ cells in the ovaries of *L. maximus* are being lost through exfoliation, they do not affect the increase in germ cell population in foetal life. Moreover, if germ cell exfoliation in *L. maximus* does contribute to the elimination of germ cells after birth as in mice and humans, it would, at most, equilibrate proliferation and loss, as no significant differences in germ cell number were found from birth to 45–60 days after birth. The persistence of a stable germ cell population from birth to 45–60 days after birth may indicate that germ-line proliferation has stopped or, if exfoliation from the surface epithelium contributes to the elimination of germ cells, a post-natal supply of new oocytes and primordial follicles could avoid the decline of germ cell population. In support of this, we found that the 60-day-old post-natal ovaries of *L. maximus* still have a remnant population of non-follicular germ cells of about 120 000 (cf. Tables 1 and 2). An alternative explanation to the presence of germ cells in the surface epithelium supports the idea that they are a source of new oocytes that could replenish the primordial oocyte pool in mice after birth (Johnson *et al*. 2004). However, this proposal is a matter of current debate with different studies presenting evidence claiming for and against the existence of *de novo* oogenesis (Tilly *et al*. 2009, Gougeon 2010). *De novo* oogenesis has been reported in several species of lorises (Butler & Juma 1970, David *et al*. 1974) in which nests of dividing oogonia persist in the adult ovary. It has been claimed that this may represent an isolated phenomenon of some prosimian species as such germ cell nests do not seem to occur in the adult ovary in rodents (Kerr *et al*. 2006). Our results support the idea that oocyte renewal may take place after birth in the South American rodent *L. maximus*. This needs further exploration, especially considering that this rodent displays massive ovulation, releasing up to 800 oocytes in each oestrus cycle accompanied by a considerable number of non-ovulated oocytes remaining in luteinising unruptured follicles (Weir 1971*a*, Jensen *et al*. 2006). Moreover, pre-ovulatory follicles are formed during gestation, and there seems to be an ovulatory process at mid-gestation with massive formation of secondary corpora lutea (Jensen *et al*. 2006, 2008) and reproductive life spans over 10 years (Weir 1971*a*). In such a dynamic ovary, *de novo* oogenesis may well account for the need of permanently rebuilding the tissue organisation and germ cell supply.

Recently, evidence has been gathered that autophagy may act as a death mechanism in the mammalian ovary (De Felici *et al*. 2008, Rodrigues *et al*. 2009, Tingen *et al*. 2009). No studies analysing autophagy in *L. maximus*
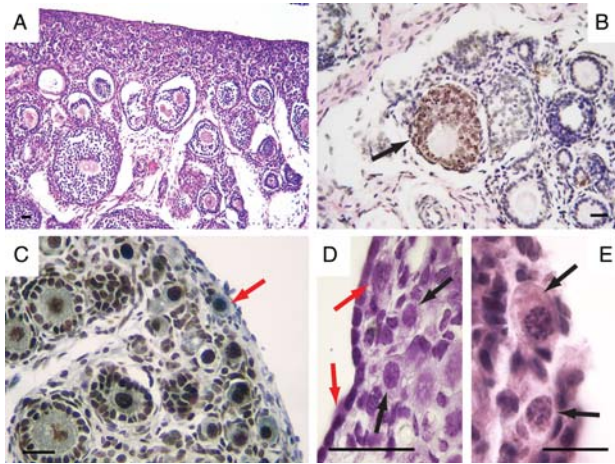
Figure 3 Germ-line development in the post-natal pre-pubertal ovary of *Lagostomus maximus*. (A) Illustrative histological section of the post-natal (45–60 days old) ovary showing the resting reserve of primordial follicles distributed in the cortex and primary, secondary and early-antral follicles that entered the growing pool. (B) Apoptosis in post-natal ovary was rare and involved early-antral follicles (arrow). (C) Detail of the surface epithelium in the post-natal ovary showing remnant oogonia (red arrow), nearest to the surface, positive for cytoplasmic VASA (blue staining) and PCNA (sharp brown nuclear staining). Note the proliferative state of granulosa cells (PCNA staining) in the primary and secondary oocytes that entered the growing pool. (D) Non-follicular oogonia-like cells near the surface epithelium (red arrows) and oogonia-like cells starting to contact somatic cells (black arrows) that do not exhibit the typical chromatin configuration of the different stages of prophase I (cf. Fig. 4I), indicating that they did not enter meiosis. (E) Detail of primary oocytes located in the cortex of the post-natal ovary showing characteristic chromatin staining of prophase I (arrows); the oocyte indicated by the upper arrow shows a leptotene configuration and somatic pre-granulosa cells just beginning to associate; the oocyte indicated by the lower arrow shows a diplotene configuration forming an incipient primordial follicle surrounded by a few squamous pre-granulosa cells. (A, D and E) Haematoxylin–eosin staining; (B) POD-converted TUNEL assay, counterstained with haematoxylin and (C) double-immunostaining for VASA and PCNA. Bar, 20 μm.

are still available. However, as has been discussed above for germ cell exfoliation, it seems unlikely that autophagy may be acting as a death mechanism that could modify the growing tendency of the germ line. Autophagy is primarily a survival mechanism to escape prolonged nutrient deprivation, but it can cause death when taken to extremes. Even if apoptosis proteins BCL2 and BCL-X$_l$ suppress autophagy by binding to beclin 1 protein, crosstalk between apoptosis and autophagy is not so simple, as autophagy can lead to cell death in collaboration with apoptosis or can help in cell survival by suppressing apoptosis, depending on the cellular environment (Zhou *et al.* 2011). In the developing ovary of the plains vizcacha, in which the *BCL2* gene exhibits sustained expression avoiding apoptosis and germ cell number increases exponentially, it seems likely that autophagy might be acting as a survival mechanism

helping to overcome nutrient limitations imposed by high proliferation.

The quantitative analysis of the different stages that germ cells go through from early development to pre-pubertal stages showed that mitotic proliferation, entrance into meiotic prophase I stage and primordial follicle formation occur as overlapping processes. It is worth noting that this pattern is comparable to female germ-line development in humans (Kurilo 1981) and
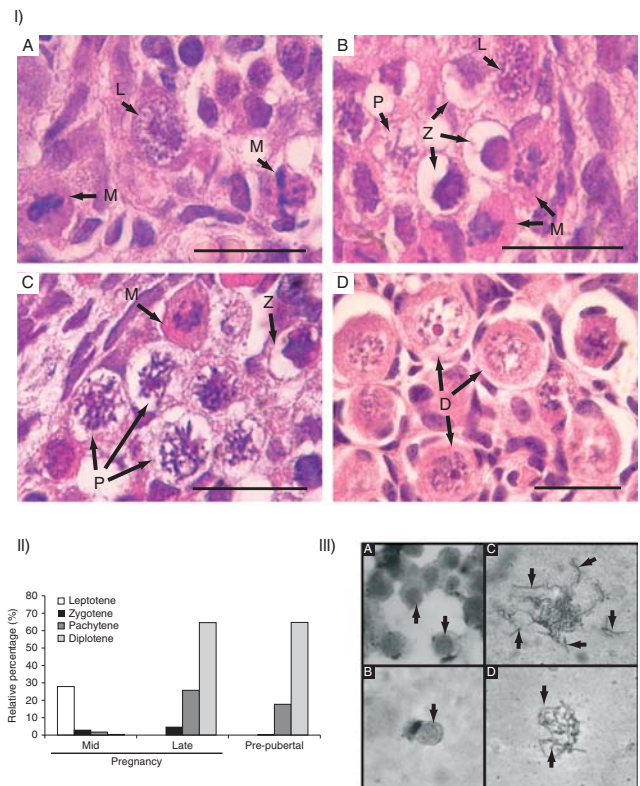
Figure 4 Morphological analysis and quantification of the progression of meiotic prophase I in the developing and perinatal ovary of *Lagostomus maximus*. (I) Prophase I stages of meiosis were identified and quantified in histological preparations by inspecting chromatin organisation. (I, A) Typical view of leptotene (L) nuclei showing heterogeneous chromatin in which chromosome condensation has started, (I, B) zygotene (Z) oocyte with an eccentrically located nucleus with sharp staining indicating full chromosome condensation, (I, C) typical view of superimposed bivalents in pachytene (P) stage and (I, D) diplotene (D) oocytes enclosed in incipient primordial follicles. M, mitotic oogonia. (II) Distribution of prophase I stages in foetal and pre-pubertal ovaries. Frequency is indicated as percentage of the total germ cell count (oogonia + oocytes + follicles). (III) Illustrative chromatin configuration in silver-stained spread preparation. (III, A) Typical view of leptotene nuclei (arrows) found in mid-developing ovary characterised by diffuse fine thread-like synaptonemal complex silver staining; (III, B) at zygotene threads thicken and become more evident (arrow). (III, C) Characteristic discrete threads (arrows) representing fully paired homologous chromosomes observed in pachytene stage in both late-gestation and pre-pubertal ovaries. (III, D) Oocyte in diplotene characterised by Y-shaped structures (lower arrow) and looped threads (upper arrow) representing the beginning of dissociation between homologous chromosomes. Bar, 20 μm.

quite different from that in rodents, in which it occurs sequentially and mostly at the perinatal stage or early after birth. The result of this pattern of germ-line development is the conformation of a post-natal ovary in *L. maximus* with a dominating quiescent primordial follicle germinal reserve and a small proportion of follicles entering the growing pool that resembles the infant human ovary (Albamonte *et al.* 2013). Although female germ lines in *L. maximus* and humans seem to follow a similar developmental pattern, intraovarian oocyte demise places them at opposite extremes, with the human ovary eliminating ∼85% of oocytes by birth (Baker 1963) and the *L. maximus* ovary showing a cumulative loss of no more than 4%, as reported herein. However, it is interesting to note that the pattern of germ cell demise through apoptosis seems to be comparable in both species, pointing to a central role of *BCL2* and *BAX* gene expression. In the human ovary, low levels of apoptosis are observed during oogonia mitotic proliferation (early gestation) due to *BCL2* expression in proliferating cells (Vaskivuo *et al.* 2001, Albamonte *et al.* 2008). At mid-gestation (weeks 18–20), when oocytes are progressing through prophase I and primordial follicle formation stages, anti-apoptotic *BCL2* stops expressing and the pro-apoptotic *BAX* gene seems to be responsible for a remarkable increase in apoptosis leading to a final cumulative 85% loss at birth (Baker 1963, Baker & Franchi 1967, Albamonte *et al.* 2008). We found a very low level of apoptosis (0.11%) in the early-developing ovaries of *L. maximus* supported by *BCL2* expression in proliferating oogonia (Leopardo *et al.* 2011). Apoptosis peaks at mid-gestation (3.62%) when oocytes enter prophase I stage and *BAX* expression becomes detectable (Leopardo *et al.* 2011). However, the low expression of pro-apoptotic *BAX* and the persistence of anti-apoptotic *BCL2* gene from mid-gestation to late gestation (Leopardo *et al.* 2011) seem to preclude an increase in the incidence of apoptosis and no more than 4% oocyte loss occurs by birth, in contrast to that observed in the human ovary. Intraovarian massive demise of germ cells through death mechanisms has been regarded as a way of eliminating oocytes exhibiting genetic defects (Tilly 2001) or exhausted germ cells acting as nurse cells to the surviving oocyte pool (Pepling & Spradling 2001) or avoiding mis-association between germ cells and somatic cells during primordial follicle formation (Guigon & Magre 2006). In any case, death and survival of the germ cell seem to be a critical balance to preclude ovarian failure and ensure viable gamete release. Then, how does *L. maximus* ensure oocyte quality if intraovarian death mechanisms are suppressed needs an in-depth investigation.

In conclusion, this study provides definitive proof that germ cell number increases continuously from early development until pre-pubertal stages in *L. maximus*, through a developmental pattern that differs from what is found in other mammals, by avoiding intraovarian massive germ cell elimination. In addition, the persistence of a considerable number of non-follicular germ cells (oogonia and primary oocytes) in the pre-pubertal ovaries provides support to a possible mechanism of follicle renewal through *de novo* oogenesis in adult life.

References

Albamonte MS, Willis MA, Albamonte MI, Jensen F, Espinosa MB & Vitullo AD 2008 The developing human ovary: immunohistochemical analysis of germ-cell specific VASA protein, *BCL-2/BAX* expression balance and apoptosis. *Human Reproduction* **23** 1895–1901. (doi:10.1093/humrep/den197)

Albamonte MI, Albamonte MS, Stella I, Zucardi L & Vitullo AD 2013 The infant and pubertal human ovary: Balbiani's body associated *VASA* expression, immunohistochemical detection of apoptosis-related BCL2 and BAX proteins, and DNA fragmentation. *Human Reproduction* **28** 698–706. (doi:10.1093/humrep/des453)

Baker TG 1963 A quantitative and cytological study of germ cells in human ovaries. *Proceedings of the Royal Society of London. Series B, Biological Sciences* **158** 417–433. (doi:10.1098/rspb.1963.0055)

Baker TG & Franchi LL 1967 The fine structure of oogonia and oocytes in human ovaries. *Journal of Cell Science* **2** 213–224.

Butler H & Juma MB 1970 Oogenesis in an adult prosimian. *Nature* **226** 552–553. (doi:10.1038/226552a0)

Byskov AG & Rasmussen G 1973 Ultrastructural studies of the developing follicle. In *The Development and Maturation of the Ovary and its Function*, pp 55–62. Ed. H Peters. Amsterdam: Excerpta Medica.

CCAC 2002 Guía para el cuidado y uso de animales de laboratorio, Mexican edition. Ottawa, ON, Canada: National Academy Press.

CCAC 2003 Guidelines on: the care and use of wildlife. Ottawa, ON, Canada: National Academy Press.

Coucouvanis EC, Sherwood SW, Carswell-Crumpton C, Spack EG & Jones PP 1993 Evidence that the mechanism of prenatal germ cell death in the mouse is apoptosis. *Experimental Cell Research* **209** 238–247. (doi:10.1006/excr.1993.1307)

David GF, Anand Kumar TC & Baker TG 1974 Uptake of tritiated thymidine by primordial germinal cells in the ovaries of the adult slender loris. *Journal of Reproduction and Fertility* **41** 447–451. (doi:10.1530/jrf.0.0410447)

De Felici M 1999 Bcl-2 and Bax regulation of apoptosis in germ cell during prenatal oogenesis in the mouse embryo. *Cell Death and Differentiation* **6** 908–915. (doi:10.1038/sj.cdd.4400561)

De Felici M, Klinger FG, Farini D, Scaldaferri ML, Iona S & Lobascio M 2005 Establishment of oocyte population in the fetal ovary: primordial germ cell proliferation and oocyte programmed cell death. *Reproductive Biomedicine Online* **10** 182–191. (doi:10.1016/S1472-6483(10)60939-X)

De Felici M, Lobascio AM & Klinger FG 2008 Cell death in fetal oocytes: many players for multiple pathways. *Autophagy* **4** 240–242.

Espinosa MB, Fraunhoffer NA, Leopardo NP, Vitullo AD & Willis MA 2011 The ovary of *Lagostomus maximus* (Mammalia, Rodentia): an analysis by confocal microscopy. *Biocell* **35** 37–42.

Flamini MA, Barbeito CG, Gimeno EJ & Ortionsky EL 2009 Histology, histochemistry and morphometry of the ovary of the adult plains vizcacha (*Lagostomus maximus*) in different reproductive stages. *Acta Zoologica* **90** 390–400. (doi:10.1111/j.1463-6395.2008.00386.x)

Flaws JA, Hirshfield AN, Hewitt JA, Babus JK & Furth PA 2001 Effect of Bcl-2 on the primordial follicle endowment in the mouse ovary. *Biology of Reproduction* **64** 1153–1159. (doi:10.1095/biolreprod64.4.1153)

Forabosco A, Sforza C, De Pol A, Vizzotto L, Marzona L & Ferrario VF 1991 Morphometric study of the human neonatal ovary. *Anatomical Record* **231** 201–208. (doi:10.1002/ar.1092310208)

Gavrieli Y, Sherman Y & Ben Sasson SA 1992 Identification of programmed cell death *in situ* via specific labeling of nuclear DNA fragmentation. *Journal of Cell Biology* **119** 493–501. (doi:10.1083/jcb.119.3.493)

Gougeon A 2010 La nèo-ovogènèse spontanée dans l'ovaire adulte est-elle une hypothèse réaliste? *Gynécologie, Obstétrique & Fertilité* **38** 398–401. (doi:10.1016/j.gyobfe.2010.04.013)

Guigon CJ & Magre S 2006 Contribution of germ cells to differentiation and maturation of the ovary: insights from models of germ cell depletion. *Biology of Reproduction* **74** 450–458. (doi:10.1095/biolreprod.105.047134)

Gundersen HJ 1986 Stereology of arbitrary particles. A review of unbiased number and size estimators and the presentation of some new ones, in memory of William R. Thompson. *Journal of Microscopy* **143** 3–45. (doi:10.1111/j.1365-2818.1986.tb02764.x)

Gundersen HJ & Jensen EB 1987 The efficiency of systematic sampling in stereology and its prediction. *Journal of Microscopy* **147** 229–263. (doi:10.1111/j.1365-2818.1987.tb02837.x)

Gundersen HJ, Bagger P, Bendtsen TF, Evans SM, Korbo L, Marcussen N, Møller A, Nielsen K, Nyengaard JR, Pakkernberg B et al. 1988 The new stereological tools: disector, fractionator, nucleator and point sampled intercepts and their use in pathological research and diagnosis. *Acta Pathologica, Microbiologica, et Immunologica Scandinavica* **96** 857–881. (doi:10.1111/j.1699-0463.1988.tb00954.x)

Hartoft-Nielsen ML, Rasmussen AK, Feldt-Rasmussen U, Buschard K & Bock T 2005 Estimation of number of follicles, volume of colloid and inner follicular surface area in the thyroid gland of rats. *Journal of Anatomy* **207** 117–124. (doi:10.1111/j.1469-7580.2005.00442.x)

Hirshfield AN 1991 Development of follicles in the mammalian ovary. *International Review of Cytology* **124** 43–101. (doi:10.1016/S0074-7696(08)61524-7)

Hiura M & Fujita H 1977 Electron microscopy observations on the epithelium of the oocyte through the peritoneal epithelium in the neonatal mouse ovary. *Cell and Tissue Research* **182** 73–79. (doi:10.1007/BF00222055)

Howell WM & Black DA 1980 Controlled silver-staining of nucleolus organizer regions with a protective colloidal developer: a 1-step method. *Experientia* **36** 1014–1015. (doi:10.1007/BF01953855)

Hsueh AJ, Eisenhower K, Chun SY, Hsu SY & Billig H 1996 Gonadal cell apoptosis. *Recent Progress in Hormone Research* **51** 433–455.

Jensen FC, Willis MA, Albamonte MS, Espinosa MB & Vitullo AD 2006 Naturally suppressed apoptosis prevents follicular atresia and oocyte reserve decline in the adult ovary of *Lagostomus maximus* (Rodentia, Caviomorpha). *Reproduction* **132** 301–308. (doi:10.1530/rep.1.01054)

Jensen FC, Willis MA, Leopardo NP, Espinosa MB & Vitullo AD 2008 The ovary of the gestating South American plains vizcacha (*Lagostomus maximus*): suppressed apoptosis and corpora lutea persistence. *Biology of Reproduction* **79** 240–246. (doi:10.1095/biolreprod.107.065326)

Johnson J, Canning J, Kaneko T, Pru JK & Tilly JL 2004 Germline stem cells and follicular renewal in the postnatal mammalian ovary. *Nature* **428** 145–150. (doi:10.1038/nature02316)

Kerr JB, Duckett R, Myers M, Mladenovska T & Findlay K 2006 Quantification of healthy follicles in the neonatal and adult mouse ovary: evidence for maintenance of primordial follicle supply. *Reproduction* **132** 95–109. (doi:10.1530/rep.1.01128)

Kim MR & Tilly JL 2004 Current concepts in Bcl-2 family member regulation of female germ cell development and survival. *Biochimica et Biophysica Acta* **1644** 205–210. (doi:10.1016/j.bbamcr.2003.10.012)

Knudson CM, Tung KS, Tourtellotte WG, Brown GA & Korsmeyer SJ 1995 Bax-deficient mice with lymphoid hyperplasia and male germ cell death. *Science* **270** 96–99. (doi:10.1126/science.270.5233.96)

Kurilo LF 1981 Oogenesis in antenatal development in man. *Human Genetics* **57** 86–92. (doi:10.1007/BF00271175)

Leopardo NP, Jensen FC, Willis MA, Espinosa MB & Vitullo AD 2011 The developing ovary of the South American plains vizcacha, *Lagostomus maximus* (Mammalia, Rodentia): massive proliferation with no sign of apoptosis-mediated germ cell attrition. *Reproduction* **141** 633–641. (doi:10.1530/REP-10-0463)

Mossman HW & Duke KL 1973 Comparative morphology of the mammalian ovary. pp 1-461 Madison, WI, USA: University of Wisconsin Press.

Motta PM, Makabe S & Nottola SA 1997 The ultrastructure of human reproduction. I. The natural history of the female germ cell: origin, migration and differentiation inside the developing ovary. *Human Reproduction Update* **3** 281–295. (doi:10.1093/humupd/3.3.281)

Motta PM, Nottola SA, Familiari G, Makabe S, stallone T & Macchiarelli G 2003 Morphodynamics of the follicular–luteal complex during early ovarian development and reproductive life. *International Review of Cytology* **223** 177–288. (doi:10.1016/S0074-7696(05)23004-8)

Myers M, Britt KL, Wreford NG, Ebling FJ & Kerr JB 2004 Methods for quantifying follicular numbers within the mouse ovary. *Reproduction* **127** 569–580. (doi:10.1530/rep.1.00095)

Pearl R & Schoppe WF 1921 Studies on the physiology of reproduction in the domestic fowl. *Journal of Experimental Zoology* **34** 101–111. (doi:10.1002/jez.1400340107)

Pepling ME & Spradling AC 2001 Mouse ovarian germ cell cysts undergo programmed breakdown to form primordial follicles. *Developmental Biology* **234** 339–351. (doi:10.1006/dbio.2001.0269)

Peters H 1969 The development of the mouse ovary from birth to maturity. *Acta Endocrinologica* **62** 98–116. (doi:10.1530/acta.0.0620098)

Ratts VS, Flaws JA, Kolp R, Sorenson CM & Tilly JL 1995 Ablation of bcl-2 gene expression decreases the numbers of oocytes and primordial follicles established in the post-natal female mouse gonad. *Endocrinology* **136** 3665–3668. (doi:10.1210/en.136.8.3665)

Rodrigues P, Limback D, McGinnis LK, Plancha CE & Albertini DF 2009 Multiple mechanisms of germ cell loss in the perinatal mouse ovary. *Reproduction* **137** 709–720. (doi:10.1530/REP-08-0203)

Speed RM 1982 Meiosis in the foetal mouse ovary. I. An analysis at the light microscope level using surface-spreading. *Chromosoma* **85** 427–437. (doi:10.1007/BF00330366)

Sterio DC 1984 The unbiased estimation of number and sizes of arbitrary particles using the disector. *Journal of Microscopy* **134** 127–136. (doi:10.1111/j.1365-2818.1984.tb02501.x)

Tilly JL 1996*a* Apoptosis and ovarian function. *Reviews of Reproduction* **1** 162–172. (doi:10.1530/ror.0.0010162)

Tilly JL 1996*b* The molecular basis of ovarian cell death during germ cell attrition, follicular atresia, and luteolysis. *Frontiers in Bioscience* **1** 1–11.

Tilly JL 2001 Commuting the death sentence: how oocytes strive to survive. *Nature Reviews. Molecular Cell Biology* **2** 838–848. (doi:10.1038/35099086)

Tilly JL, Tilly KI & Perez GI 1997 The genes of cell death and cellular susceptibility to apoptosis in the ovary: a hypothesis. *Cell Death and Differentiation* **4** 180–187. (doi:10.1038/sj.cdd.4400238)

Tilly JL, Niikura Y & Rueda BR 2009 The current status of evidence for and against postnatal oogenesis in mammals: a case of ovarian optimism versus pessimism? *Biology of Reproduction* **80** 2–12. (doi:10.1095/biolreprod.108.069088)

Tingen CM, Bristol-Gould SK, Kiesewetter SE, Wellington JT, Shea L & Woodruff TK 2009 Prepubertal primordial follicle loss in mice is not due to classical apoptotic pathways. *Biology of Reproduction* **81** 16–25. (doi:10.1095/biolreprod.108.074898)

Vaskivuo TE, Anttonen M, Herva R, Billig H, Dorland M, te Velde ER, Stenbäck F, Heikinheimo M & Tapanainen JS 2001 Survival of human

ovarian follicles from fetal to adult life: apoptosis, apoptosis-related proteins, and transcription factor GATA-4. *Journal of Clinical Endocrinology and Metabolism* **86** 3421–3429. (doi:10.1210/jc.86.7.3421)

Weir BJ 1971*a* The reproductive physiology of the plains vizcacha, *Lagostomus maximus. Journal of Reproduction and Fertility* **25** 355–363. (doi:10.1530/jrf.0.0250355)

Weir BJ 1971*b* The reproductive organs of the female plains viscacha, *Lagostomus maximus. Journal of Reproduction and Fertility* **25** 365–373. (doi:10.1530/jrf.0.0250365)

Wordinger R, Sutton J & Brun-Zinkernagel AM 1990 Ultrastructure of oocyte migration through the mouse ovarian surface epithelium during neonatal development. *Anatomical Record* **227** 187–198. (doi:10.1002/ar.1092270207)

Zuckerman S 1951 The number of oocytes in the mature ovary. *Recent Progress in Hormone Research* **6** 63–109.

Zhou F, Yang Y & Xing D 2011 *Bcl-2* and *Bcl-xL* play important roles in the crosstalk between autophagy and apoptosis. *FEBS Journal* **278** 403–413. (doi:10.1111/j.1742-4658.2010.07965.x)